**Proceedings of ASME Turbo Expo 2026**
**Turbomachinery Technical Conference and Exhibition**
**GT2026**
**June 15-19, 2026, Milan, Italy**

# GT2026-177871

# IMPACT OF INLET FLOW PULSATIONS ON PERFORMANCE OF CENTRIFUGAL COMPRESSORS AND IMPACT ON ITS DESIGN

**Simon Stummann  Matthias Schleer  Shreman Parikh**
Howden Turbo GmbH, a Chart Industries Company
Frankenthal, Germany

## ABSTRACT

*Ocean-going vessels with two-stroke engines require exhaust gas recirculation (EGR) systems to mitigate emissions. These systems based in the exhaust of the main engine incorporate EGR compressors operating under significant pulsating inlet flow conditions. Stage measurements indicate a lower mass flow under transient pulsating conditions compared to steady flow conditions. This paper investigates the underlying effects using steady and transient computational fluid dynamics (CFD) simulations. The transient averaged losses of the subcomponents' diffuser and volute are higher than the losses of a comparable steady state design point. This transient behavior can be generalized on compressor design. Based on these findings design rules are developed and used for a future generation of EGR compressors. These are evaluated on subcomponent stability and transient loss behavior. Both generations are compared, and the improved behavior of the second generation is demonstrated through steady and transient CFD simulations. The paper concludes with general design rules derived from the analysis, providing insights into future EGR compressor designs to enhance performance and reliability under varying flow conditions.*

Keywords: radial compressor, pulsating flow

## NOMENCLATURE

*Roman letters*

| | |
|---|---|
| D | Diameter |
| $\dot{m}$ | Mass flow |
| p | Pressure |
| h | Enthalpy |
| T | Temperature |
| t | Time |
| u | Circumferential velocity |
| y+ | Non dimensional wall distance |

*Greek letters*

| | |
|---|---|
| $\alpha$ | Alpha (flow angle) |
| $\rho$ | Density |
| $\pi$ | Pressure ratio |
| $\omega$ | Loss coefficient |
| $\Psi$ | Non-Dimensional Volume flow |
| $\Psi_p$ | Pressure stability criteria |
| $\Psi$ | Non-dimensional enthalpy rise |

*Subscripts*

| | |
|---|---|
| DP | Design point |
| Surge | Last stable near surge operation point |
| t | Total / stagnation values |
| s | Static values |
| norm | Normalized value by main operation point |
| red | Reduced value |
| volute | Volute |
| 1 | Impeller inlet |
| 2 | Impeller outlet / diffuser inlet |
| 4 | Diffuser outlet / volute inlet |
| 5 | Volute and compressor outlet |

*Acronyms and definitions*

| | |
|---|---|
| CFD | Computational Fluid Dynamics |
| EGR | Exhaust Gas Recirculation |
| | |
| IMO | International maritime organization |
| NOx | Nitrogen Oxides |
| RANS | Reynolds-Averaged-Navier-Stokes |
| | |
| Compressor | System out of impeller, diffuser and volute |
| Impeller | Rotor only |
| EGR GEN1 | first generation of EGR compressors |
| EGR GEN2 | second generation of EGR compressors |

## 1. INTRODUCTION

Two-stroke engines play a crucial role in marine propulsion, particularly for large ocean-going vessels. These engines are favored over their four-stroke counterparts for several reasons, higher efficiency, higher power per size due to their larger stroke and fuel flexibility, burning low-grade fuel oils. Countries with large ports and coastlines have a particular interest in lowering the emissions. They aim to reduce fuel consumption and emissions, especially NOx emissions. These emissions are regulated by international standards, particularly the IMO Tier III regulations [1]. This standard is already applied in the national waters of the USA and Baltic Sea and is planned for other sea areas such as the Mediterranean, China and Australia. The preferred way to reduce NOx emissions is by exhaust gas recirculation (EGR). EGR enables the Tier III requirements without additional exhaust gas aftertreatment. Furthermore, EGR works for both fuel oil and gas engines [3]. This also reduces gas or fuel oil consumption by 3-5%. The EGR system operates by drawing around 30-50% of the engine's exhaust gas into the EGR receiver. There, the gas first passes through a pre-spray stage to reduce its temperature, followed by a water mist catcher to remove residual moisture. The conditioned gas is then compressed by the EGR compressor—highlighted in this study—to raise its pressure back to the scavenging-air level before being reintroduced into the engine [2].

The first generation of EGR compressors [4] were designed using well known steady state design rules on the main operation range matching several possible ship engines with different operation points. These compressors are well proven in operation for several years. Nevertheless, field measurements indicate that EGR GEN1 compressors experience a reduction in mass under pulsating conditions compared with steady state test bench measurements. This indicates that steady state design is not fully sufficient for the design of such a compressor. In exceptional operation points these pressure pulsations can be as high as the stage pressure rise itself. With these presence of these inlet pulsations steady state design rules fail to deliver sufficient results. Hence, the flow pulsations were addressed in the design project shown in this paper.

Time constant inlet distortions like secondary flows from upstream pipes [5] have an impact on performance and are widely discussed in several papers and their significance well known. The significance of pressure pulsations from two- or four-stroke engine exhausts are well analyzed for turbochargers turbine inlets [6] and [7] with significant influence on performance and hence also flow geometry. A major numerical study [8] on pulsations shows the significancy of induced secondary flow and the effect on performance. Little is known about the aerodynamics of compressors in regards of pulsating flows. The main interest there lies in the interaction of (turbocharger) compressors with downstream engines. The focus in volute flow is approached in [9]. In the volute, the fluctuating mass flow induces a backflow region near the volute tongue. The surge frequency of compressor is also varying with a pulsating outlet pressure [10].

The main objective of the work is to design a new generation of EGR compressors. These compressors are attached to more powerful engines with a need for higher mass flow. At the same time each compressor deals with significant pressure fluctuations at the inlet.

In this context this paper evaluates the unsteady compressor interactions due to inlet pressure pulsations and shows the unsteady design process of the new EGR compressor generation. This is interesting, since it shows how unsteady pressure fluctuations work in a radial compressor. It is furthermore shown how the volute as a circumferential non-homogenous part interacts with the pulsations.

## 2. METHODOLOGIES

The compressor was designed using in-house tools for both the impeller and the volute. The designs were evaluated through steady-state CFD simulations using Ansys CFX, conducted at both maximum rotational speed and two-thirds of the maximum speed. Several steady state optimization cycles were performed during the design process. The primary objective during this phase was to align the main operating points with an extended flow range and pressure rise.

The initial design of the first-generation EGR GEN1 compressor was derived from a conventional high-pressure radial compressor featuring slightly backward-curved blades. The diffuser was configured according to established design principles aimed at maximizing pressure recovery, as described in [11]. Both the first and second generations utilize the same electric motor, thereby operating under identical constraints of maximum rotational speed and torque. The second-generation EGR GEN2 configuration was developed based on insights gained from the analysis of flow pulsations, incorporating blades with a pronounced backward curvature. Additionally, the diffuser underwent a complete redesign informed by the findings presented in this study.

### 2.1 Steady and Transient CFD-RANS Simulations

The pre-design was performed using steady-state CFD RANS simulations. The evaluations of pressure pulsations and the final design were done with the help of unsteady simulations. The time of one pulse traveling through the compressor varies due to the collection of mass inside the circumferentially inhomogeneous volute and additionally several pulses are simultaneously inside the compressor. Hence, several pulses are calculated.

The simulated geometry consists of an inlet section, which is designed according to the real compressor inlet. Attached to the inlet is the impeller followed by the diffuser and the volute including an outlet section. Between inlet and impeller is an interface as well as between impeller and vaneless diffuser. The computational domain for EGR GEN 1 is shown in figure 1.

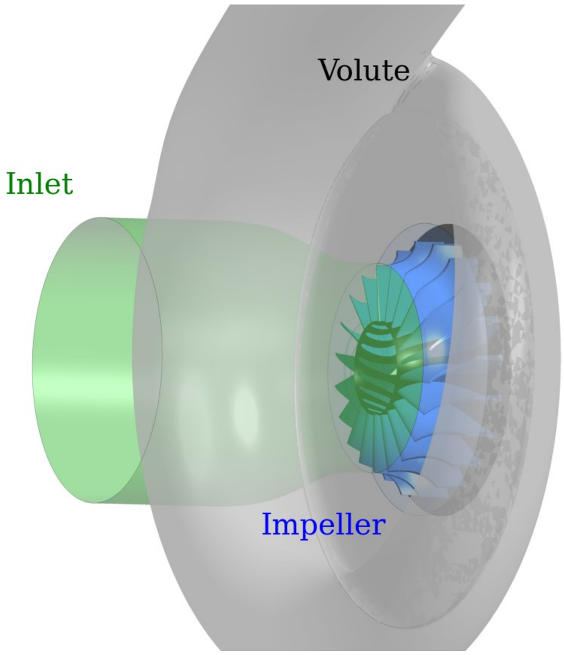


**Figure 1:** COMPUTATIONAL DOMAIN FOR EGR GEN1

The meshing was performed using Ansys TurboGrid for the impeller and Ansys meshing for the inlet and volute section. The Inlet has 0.6 m. cells, one impeller blade consists of 1.2 m. cells with more than 21 cell layers inside the tip gap. The volute consists of 2.5 m. cells. All wall surfaces have a Y+ of 1. The meshing has a quite high resolution outside the boundary layers to capture unsteady effects in the transient simulations. Steady state simulations were performed at the same mesh.

**Physical models, Turbulence and solver settings**

The simulations are conducted under the assumption that the working fluid behaves as an ideal gas. The total energy equation, including the viscous work term, are solved to account for the energy contributions from both the flow and viscous dissipation. A high-resolution upwind scheme of second order is employed for the advection terms. The turbulence is modeled using a high-resolution approach to capture the intricate details of turbulent flow structures. The Menter Shear Stress Transport (SST) model is employed for turbulence closure. The SST model combines the advantages of the ($k$-ω) model in the near-wall region with the ($k$-ε) model in the far-field, providing a robust and accurate prediction of turbulence effects across different flow regimes. Steady-state simulations are conducted with mixing planes positioned between the inlet and impeller, as well as between the impeller and diffuser. Periodic interfaces are applied at the inlet and between two blades.

Transient simulations utilize the Second Order Backward Euler model. These simulations incorporate a complete inlet and impeller model with all blades discretized. All interfaces are changed to transient interfaces. At the specified speed, 7.5 revolutions occur per pulse. During the transient state, 30 time steps are executed per blade passing of EGR_GEN1, equating to 600 time steps per revolution and 4500 time steps per pulse. This leads to a time step of 1.38e-5s. The EGR_GEN2 with 9 blades is simulated with the same time step. Initially, three revolutions with constant total inlet pressure are simulated. Then two pulses or 15 revolutions are calculated before starting averaging and writing out results. Subsequently, the simulations are averaged over two pulses, corresponding to 15 revolutions, resulting in an averaging phase of 9000-time-steps. Averaging was carried out on primary calculated quantities and secondary quantities like loss coefficients were subsequently calculated from them.

**Boundary conditions**

As inlet boundary conditions, the total pressure and static temperature were applied. Additionally, a flow vector perpendicular to the inlet area, corresponding to the open area inflow, was utilized. These values were derived from test bed measurements. The turbulence level, not determined from measurements, was selected based on empirical experience, assuming a medium level of turbulence. For the transient simulations, the total inlet pressure boundary condition was adjusted to a time-dependent function, corresponding to the given motor frequency. For both steady and transient simulations, the static outlet pressure was maintained as a constant, representing a larger outlet volume, specifically the motor induction tract.

**Verification and Validation**

Standard steady convergence criteria like residuals of mass, momentum and turbulence, as well as balances of these values were used. Additionally, the convergence of variables of interest like efficiency, pressure ratio, mass flow, and torque are observed. For unsteady convergence a setup according to [11] was implemented by comparing main frequencies and different pulses against each other. The unsteady fluctuations were observed for blade passing and inlet pressure fluctuations and compared to previous timesteps respective pulsations. This was done using monitor points as well as averaged values at inlet, interfaces and outlet. The baseline first generation Exhaust Gas Recirculation compressor was measured under steady-state conditions, and the results were compared to those from a steady-state CFD. The discrepancies in mass flow, pressure ratio, and efficiency were all found to be below 1%, that can be compared in figure 3. Additionally, a mesh refinement study was conducted by increasing the mesh density by a factor of 8 and comparing the steady-state simulations. No significant differences were observed.

## 2.2 Investigated Design Points

For the steady-state design, several speed lines were analyzed. Transient simulations were carried out using one operation point at high loaded conditions near surge. At this near-surge operating point the steady state surge margin is within 10% of maximum pressure rise. While implementing the pulsations, the specified transient total-to-static pressure ratio fluctuated between the stable and unstable operation. Based on the maximum pulsating pressure rise the surge margin becomes with -15% partly negative. Hence, a steady state operating compressor would run in surge at these conditions. Both EGR generations were simulated with the same surge margin to have a comparable flow field.

## 2.3 Pulsating Flow Characteristics

The designated two-stroke engine operates at different loads with different rotational speeds and motor loading. In general, the pulse frequency is the product of motor speed multiplied with the number of cylinders. For two stroke engines there is one pulse per rotation. The pulses are essentially mass flow pulses coming from the exhaust of the motor [6], [7]. The shape of one flow pulse was designed according to [6], [7] and [8] with a sharp incline and a not so sharp decline with a time frame of almost no flow before the next pulse. For all cylinders these pulses were overlapped with different phase angles according to the different crank shaft positions. For the whole operation range, the pulse frequency is significantly lower than the compressor frequency. For example, a motor having 12 cylinders at a speed of 80rpm during full load operating condition. That means the compressor inlet is exposed to a pulse frequency of 16Hz. The average residence time of a fluid particle within the compressor is approximately 0.05 seconds. This duration is comparable to the period of a single pulsation cycle (0.06 seconds), and significantly exceeds the time required for one full compressor rotation (0.00633 seconds). Consequently, the pulsation cannot be classified as a quasi-steady phenomenon characterized by varying operating points, nor can it be attributed to conventional unsteady effects associated with blade passing frequencies. Despite not fitting into these typical categories of unsteadiness, the influence of pulsation is non-negligible and must be accounted for in the analysis of compressor performance and flow behavior. The inlet pulsations shown in figure 2 were applied on the transient simulation after three impeller rotations transient initialization. First a decrease in inlet total pressure was applied, leading the compressor closer or in the instability/ surge region. Then with increasing pressure the compressor is stabilized to an inlet pressure maximum higher than the steady state inlet pressure.

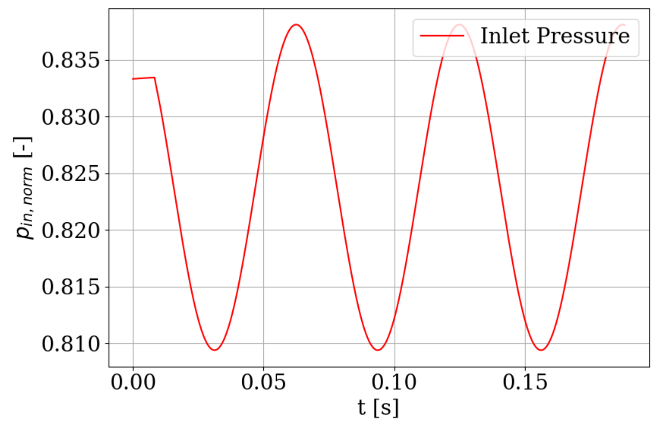


**FIGURE 2**: TIME TRANSIENT, PULSATING INLET BOUNDARY CONDITION

## 3. RESULTS AND DISCUSSION

### 3.1 Steady Design

In figure 3 are the reduced mass (1) flow and total pressure ratio (2) speed lines shown based on steady state results.

$$\dot{m}_{red} = \frac{\dot{m}_1 \sqrt{T_{t1}}}{p_{t1}} \quad (1)$$

$$\Pi_{tt} = \frac{p_{t4}}{p_{t1}} \quad (2)$$

Both speed lines are shown at the same maximum rotational speed, with EGR GEN2 at a higher tip speed due to its bigger diameter. Compared to EGR GEN1 (green) the new EGR GEN2 (blue) compressor has significantly higher mass flow and a higher maximum total pressure ratio, shown in figure 3. With these, the second generation achieves the primary design goals. Additional to that, the isentropic efficiency of EGR GEN2 is significantly increased, and the point of best efficiency has moved to higher mass flows, which corresponds to the need for a reduced torque to match the same motor. Both compressor generations were experimentally measured on the in-house testbed. The overall performance indicates a strong correlation between steady-state numerical predictions and experimental measurements. For EGR GEN1, the maximum pressure ratio near the surge limit exhibits good agreement between computational and experimental data. In contrast, for EGR GEN2, the experimentally determined surge point occurs at a significantly higher pressure ratio compared to the steady-state numerical prediction.

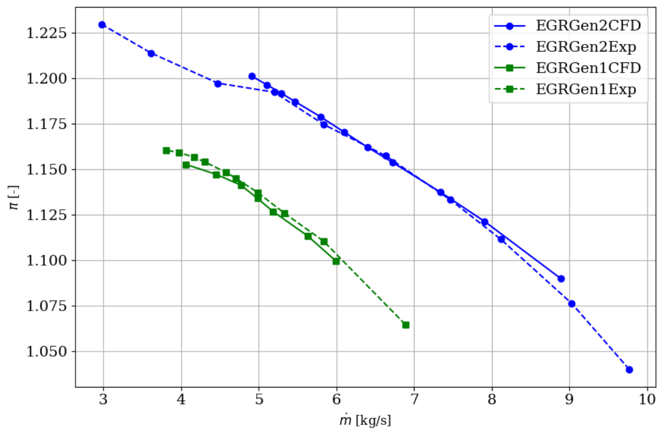


**FIGURE 3:** STEADY STATE CFD PERFORMANCE MAP VS: STEADY STATE MEASUREMENTS

The static pressure rise along the meridional axis reveals significant differences between the two generations of EGR, as illustrated in figure 4. In this figure meridional position 1 is the impeller inlet, position 2 the impeller outlet and position 3 the diffuser outlet. EGR GEN1 (green) is configured as a compressor, characterized by a low static pressure rise within the impeller. Consequently, the diffuser of EGR GEN1 is responsible for approximately 50% of the total static pressure rise. Initially, the diffuser exhibits a steep pressure gradient, which subsequently levels off to an almost horizontal profile that indicates that the maximum possible pressure rise in the diffuser is reached. In contrast, EGR GEN2 (blue) is designed with compressor-like characteristics, achieving a high static pressure rise within the impeller that accounts for nearly the entire required static pressure rise. The diffuser in EGR GEN2 contributes only about 8% to the pressure rise, maintaining a steady and constant pressure increase throughout.

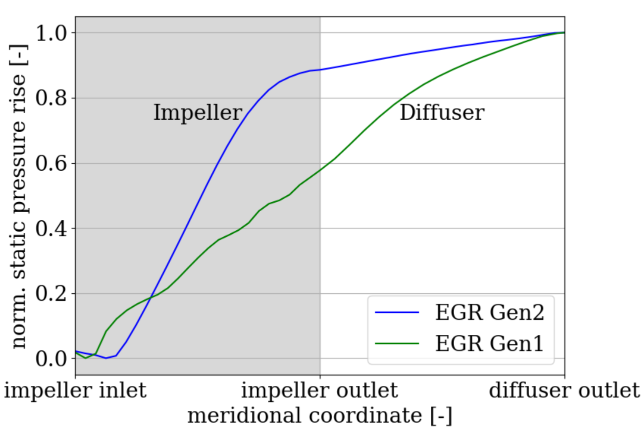


**FIGURE 4:** MERIDIONAL PRESSURE RISE OF EGR GEN1 AND EGR GEN2

### 3.2 Subcomponent Stability Characteristics

To determine unstable subcomponents of the compressor the method developed in [13], [14], [15] is used. The subcomponent pressure rise characteristics (3) is compared to the reduced mass flow. If the gradient of this gets positive, this component has a destabilizing effect on the compression system:

$$\Psi_p = \frac{\Delta p_s}{\rho U_2^2} \tag{3}$$

When this characteristic exhibits a positive gradient, it can be demonstrated that the associated subcomponent imposes a significant destabilizing effect on the intrinsic stability of the component, manifested as increased backflow and the integrity of the overall compression system. As a result, rotating stall phenomena may arise even under conditions where global system stability is nominally maintained [16]. As illustrated in figure 5a, both generations of impellers exhibit a negative gradient and hence a general stability over a wide operation range. The EGR GEN1 impeller (green) shows a change in stability near the surge line. In contrast, the EGR GEN2 (blue) impeller is designed to achieve a higher static pressure rise and maintains stable for all converging steady state CFD simulations.

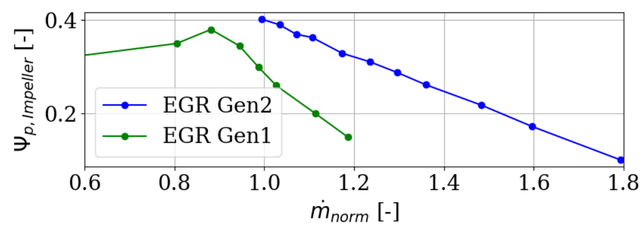


5a) Stability criterion for both impeller

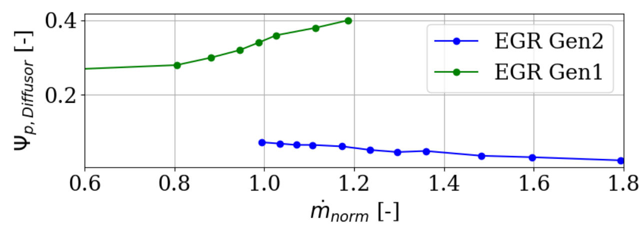


5b) Stability criterion for both diffusors

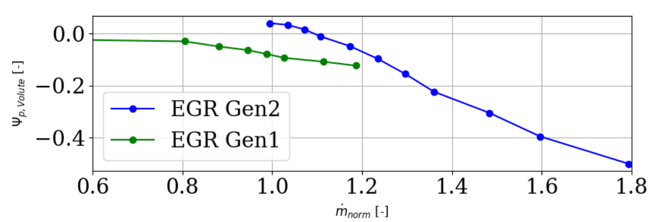


5c) Stability criterion for both volutes

**FIGURE 5:** SUBCOMPONENT FLOW STABILITY CHARACTERISTICS

The primary distinction between the two configurations lies in the diffuser shown in figure 5b). The EGR GEN1 diffuser, with a significantly higher pressure rise, exhibits a positive gradient over the whole operational range, which destabilizes the system. Conversely, the EGR GEN2 diffuser is designed with a lower pressure rise and a negative gradient to stabilize the flow. This implies that the lower static pressure at the EGR GEN1 impeller outlet is converted into a significantly higher static pressure rise within the diffuser, resulting in a generally destabilizing flow field. From a steady-state design perspective, the EGR GEN1 diffuser is likely the primary destabilizing effect of the compressor.

Both EGR GEN1 and EGR GEN2 volutes demonstrate stable performance curves in figure 5c. However, it is noteworthy that both exhibit a decline in static pressure rise EGR GEN1 in the overall stable performance area and EGR GEN2 under high flow operating conditions.

### 3.3 Transient Performance map and mass flow

Given that EGR compressors are specifically designed to operate under highly unsteady flow conditions, transient simulations were performed to capture their dynamic behavior. The corresponding results are presented below. In addition to the steady-state speed lines, figure 6 illustrates the impeller behavior at a selected operating point on the performance map. The EGR GEN1 is colored in green, the EGR GEN2 in blue and each steady state start point for the transient simulation is marked red.

It should be noted that the pressure ratio balancing in the transient analysis is not strictly accurate, as it is computed within the same time step rather than by tracking identical fluid particles from inlet to outlet. Nevertheless, this approach offers a reasonable approximation of the pulsation magnitude relative to the flow and pressure ratio.

The transient operating condition reveals a hysteresis-like trajectory. The mass flow rate fluctuates by approximately 30% relative to the steady-state value, while the pressure ratio varies by 38% of the total pressure rise. For both compressor configurations, it is evident that the instantaneous pressure ratio occasionally exceeds the maximum value observed under steady-state conditions.

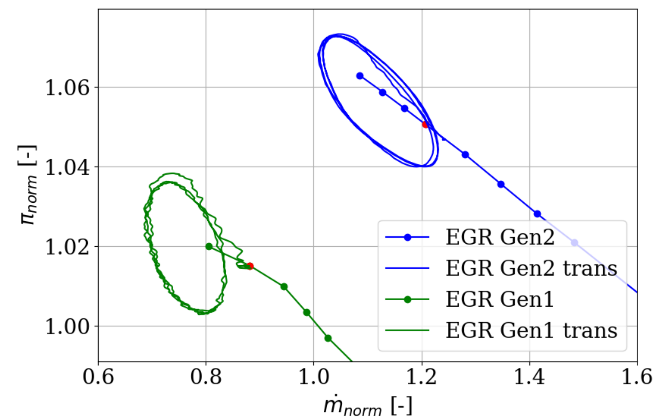


**FIGURE 6:** COMPRESSOR STEADY STATE VS. TRANSIENT PERFORMANCE MAP

Figure 7 presents the impeller performance map, illustrating the total impeller pressure ratio as a function of mass flow rate. Distinct differences between the two configurations are evident. For the EGR_GEN2 configuration, the transient performance closely follows the steady-state performance curve, exhibiting only a slightly reduced gradient. Notably, no hysteresis behavior is observed in the impeller response, suggesting that the hysteresis identified in the compressor performance map (figure 6) originates primarily from the diffuser and volute components.

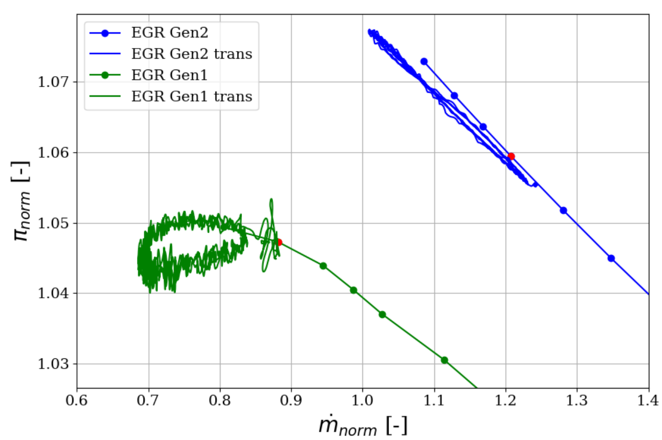


**FIGURE 7:** IMPELLER PERFORMANCE MAP (STEADY VS. TRANSIENT)

In contrast, the EGR GEN1 impeller demonstrates a pronounced hysteresis loop within its own performance characteristics. Superimposed on this overall hysteresis are additional unsteady fluctuations, indicating a more complex and dynamic response under pulsating flow conditions.

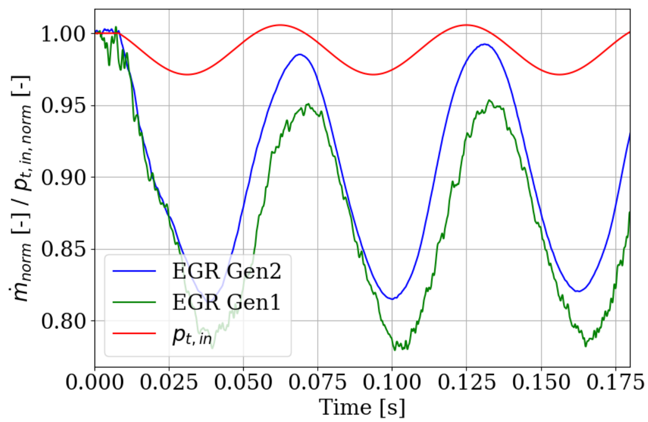


**FIGURE 8:** PULSATING NORMALIZED INLET MASS FLOW

Figure 8 illustrates the inlet mass flow rate, normalized to the steady-state value. For comparison, the normalized total inlet pressure is also presented. During the initial pressure pulse, the mass flow across all observed sections drops to approximately 80% of the steady-state value. In the subsequent rising phase, the mass flow does not fully recover to the steady-state level. Both compressor configurations then exhibit relatively stable oscillatory behavior, with flow maxima and minima remaining within a consistent range. Specifically, the EGR GEN1 configuration shows mass flow fluctuations between 78% and 95% of the steady-state value, while the EGR GEN2 configuration performs more favorably, with fluctuations ranging from 82% to 98%. It is particularly noteworthy that neither compressor configuration achieves the steady-state inlet mass flow, even during periods when the inlet pressure exceeds the steady-state level. This highlights the significant influence of pulsating flow dynamics on compressor performance, independent of inlet pressure magnitude.

### 3.4 Transient performance and mass flow losses

Both EGR compressor configurations exhibit a reduction in mass flow under pulsating conditions, suggesting a generalized underlying mechanism. A simplified explanatory approach considers the transient flow field as a superposition of quasi-steady flow states. Within this framework, the loss coefficient defined as

$$\omega = \frac{p_{t\,out} - p_{t\,in}}{p_{t\,in} - p_{in}} \tag{4}$$

is used to characterize the aerodynamic losses.

The loss coefficient typically follows a convex, parabolic characteristic with respect to mass flow (or generalized Mach number) and flow angle displayed for the volute in figure 9. The steady-state operating point lies somewhere along this curve, either at the optimum or in a suboptimal region. Under pulsating conditions, both mass flow and flow angle fluctuate, leading to corresponding fluctuations in aerodynamic losses. Even when operating at the optimal point, deviations in either direction result in increased losses.

Due to the convex nature of the loss function, the time-averaged loss coefficient under unsteady conditions is always greater than the loss at the steady-state point. This is formally supported by **Jensen's inequality** [15], which applies to convex functions. Applied to the flow coefficient, this yields:

$$\omega\big(w(\dot{m}_{steady}, alpha_{steady}\big) < \int \omega\big(\dot{m}(t), \alpha(t)\big)dt \tag{5}$$

Figure 9a illustrates the loss characteristic of a subcomponent, exemplified by a volute. The steady-state operating point is indicated by a green marker, while the operational range induced by inlet pulsations is represented by blue markers. The mean loss within this pulsating range is denoted by a red marker and as expressed in Equation (5), exceeds the steady-state loss. This observation underscores that the additional losses arising from averaging a pulsating flow are not primarily governed by the absolute loss magnitude of the subcomponent itself, but rather by the curvature of the loss curve.

Applying these increased losses of a $\Phi - \Psi$ performance map in Figure 9b using (6) and (7)

$$\Phi = \frac{4\dot{m}}{\rho \pi U_2 D_1^2} \tag{6}$$

$$\Psi = \frac{\Delta ht}{U_2^2} \tag{7}$$

The blue curve represents the theoretical performance dictated by the impeller geometry and outlet blade angle. The red curve illustrates the steady-state compressor behavior, accounting for flow losses. The gap between these two curves corresponds to the steady flow losses. The green curve depicts the performance under averaged inlet pulsations; the deviation between the green and red curves arises from the pulsation-induced averaging effect. For a given required pressure rise ($\Psi$), it becomes evident that the mass flow ($\Phi$) at the pulsation-averaged operating point (green marker) is lower than that of the steady-state curve without pulsations (red marker).

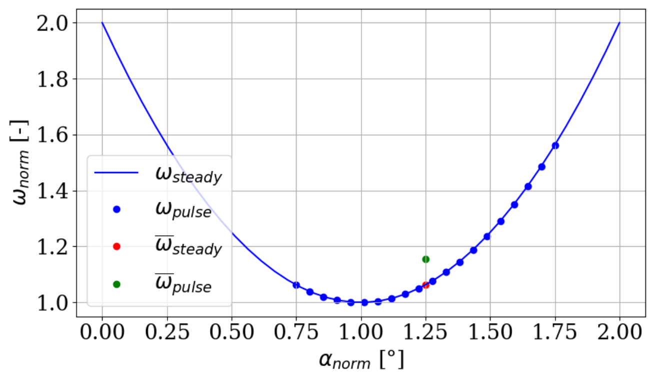


9a) Convex loss curve

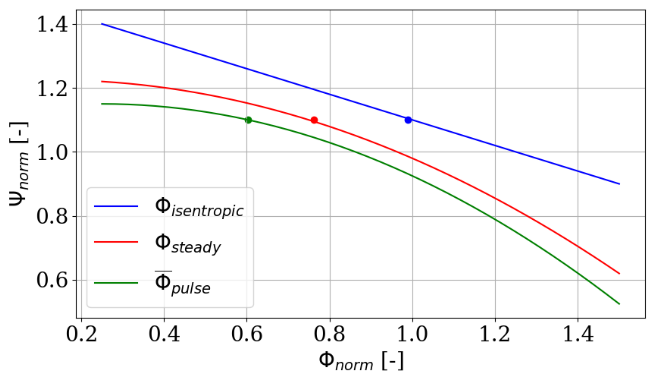


9b) Φ - Ψ diagram

**Figure 9:** EXEMPLARY LOSS CHARACTERISTIC AND $\Phi - \Psi$ DIAGRAM OF A COMPRESSOR

In both EGR compressors, the stationary components, namely the diffuser and volute, are primarily responsible for this behavior. Assuming circumferentially and spanwise homogeneous inflow conditions, the loss surface expressed as a function of mass flow and inlet flow angle exhibits a convex dependence in both dimensions, as illustrated in Figure 10.

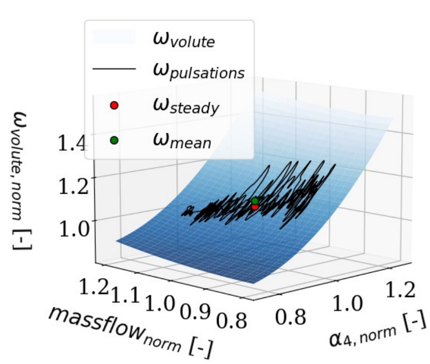


**FIGURE 10:** LOSS CHARACTERISTIC ω OF EGR_GEN1 VOLUTE

Figure 10 illustrates the loss coefficient ($\omega_{\text{Volute}}$) for a comparable at same mass flow and flow angle steady-state operating point (depicted in red), as well as the loss coefficient under pulsating conditions as a function of flow angle and mass flow (shown in black). Additionally, the time-averaged loss coefficient derived from both steady-state and transient simulations under pulsating inflow conditions is indicated in green. The results indicate that the volute of EGR GEN1 exhibits an approximately 5% higher time-averaged loss coefficient under pulsating inflow compared to steady-state conditions. This increase in losses is attributed to the convex curvature of the loss characteristic. For the diffuser, the loss characteristic exhibits an even more pronounced convex profile. Consequently, the time-averaged loss coefficient ($\omega_{\text{Diffuser}}$) increases substantially—by approximately 40%—when the compressor operates under pulsating inflow conditions compared to steady-state operation.

In contrast, the EGR GEN2 configuration demonstrates a more moderate increase: the time-averaged loss coefficients for both the diffuser and volute rise by approximately 10% compared to steady-state conditions. Although the relative increase in the volute of EGR GEN2 appears higher, its absolute loss coefficient remains comparable between EGR GEN1 and EGR GEN2.

**Impact on impeller pressure rise and mass flow**

The observed increase in pulsating flow losses has a pronounced impact on impeller performance and its capacity to maintain mass flow delivery. Given that the overall compressor total pressure rise remains constant, the impeller must compensate for the additional losses by increasing the impeller outlet total and static pressure and hence achieving a higher total pressure ratio. Since the impeller operates at a fixed rotational speed, the only viable mechanism to increase the static and total pressure at the impeller outlet is by reducing the mass flow rate.

The extent of this mass flow reduction is strongly influenced by the gradient of the performance curve. As the operating point shifts, the loss characteristics of the compressor subcomponents also evolve until a new equilibrium is established between the transient pressure rise and the associated losses at the corresponding transient mass flow rate.

This effect is particularly pronounced in the EGR GEN1 configuration, where the impeller performance curve exhibits a relatively flat, yet negative gradient. In this case, even a modest increase in total pressure loss results in a disproportionately large reduction in mass flow, on the order of 5%.

### 3.5 Comparison of transient pressure at subcomponent inlet and outlet

A more detailed understanding of pulsation effects can be achieved through an analysis of time-resolved pressure signals, as illustrated for the EGR GEN1 configuration in Figures 11a (total pressure) and 11b (static pressure). All pressure signals are normalized with respect to their corresponding steady-state values. The reference inlet pulsation, represented by the total pressure $p_t$(red), is prescribed as a boundary condition and serves as the baseline for comparison.

At the impeller outlet, the total pressure signal $p_t$(green) for EGR GEN1 exhibits a trend similar to the inlet total pressure. However, at the compressor outlet, the total pressure signal (blue) shows a significant reduction in both average value and amplitude compared to the steady-state reference. This behavior indicates increased losses within the diffuser and volute. The static pressure at the inlet (Figure 11b, red) follows the pulsating trend of the total pressure. At the impeller outlet, however, the static pressure does not follow the incoming pulsations; instead, it is truncated at approximately half the pulse amplitude. The static outlet pressure (blue) remains constant due to the imposed boundary condition.

A comparison between total pressure (Figure 11a) and static pressure (Figure 11b) at the impeller–diffuser interface (green) highlights the influence of pulsations. While the total pressure closely follows the inlet pulsations, the static pressure remains elevated. This phenomenon can be attributed to the diffuser and volute, which require a minimum pressure differential—dependent on mass flow—to overcome their inherent losses. As these losses increase under pulsating conditions, the required total pressure rise also increases.

Furthermore, the difference between total and static pressure at both the impeller outlet and compressor outlet suggests a reduction in velocity and, consequently, mass flow within the impeller. This is reflected in a slight negative slope in the impeller performance map (Figure 7). Since the impeller cannot supply the additional total pressure required to compensate for increased downstream losses, it responds by reducing mass flow.

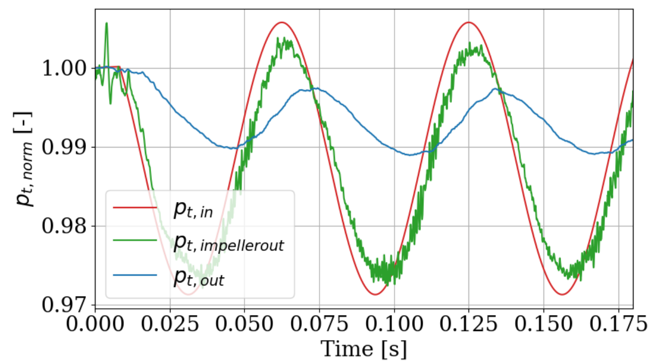


11a) EGR Gen1 Total pressure pulsations

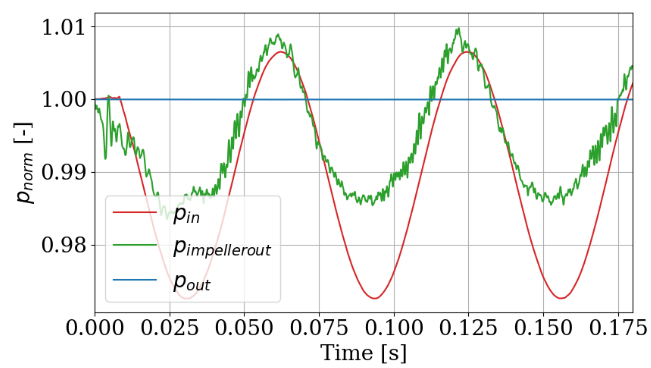


11b) EGR Gen1 Static pressure pulsations

**FIGURE 11:** EGR GEN1 NORMALIZED TOTAL PRESSURE a) AND PRESSURE b) (INLET, IMPELLER-DIFFUSER INTERFACE AND OUTLET)

In contrast, the EGR GEN2 configuration exhibits markedly different behavior under pulsating inflow conditions. Figure 12 presents the time-resolved total a) and static pressure b) signals, respectively, for the EGR GEN2 configuration, revealing similar but more favorable characteristics compared to EGR GEN1.

The outlet total pressure signal (12a - blue) exhibits significantly higher values than those observed in EGR GEN1, indicating improved impeller performance and lower losses under pulsating conditions. At the impeller outlet (green), the static pressure is quite similar to the behavior in EGR GEN1, while the total pressure 12a) green is elevated. The elevation exists compared to the total inlet pressure, Figure 12a red and compared to EGR GEN1, Figure 11a). This confirms the two effects, first the hypothesis that higher downstream losses lead to a rise in upstream total pressure. Additionally, the impeller of EGR GEN2 can deliver additional total pressure rise with a steeper gradient, shown in Figure 7.

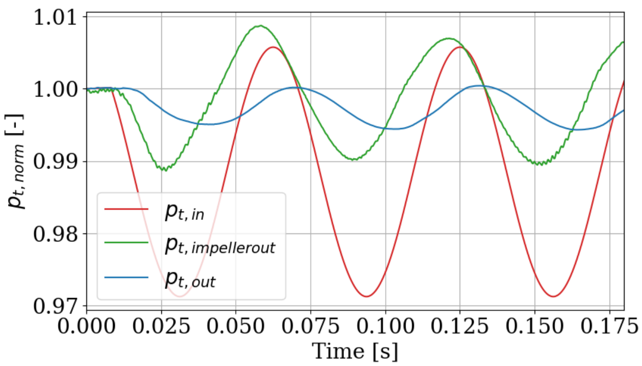


12a) EGR Gen2 Total pressure pulsations

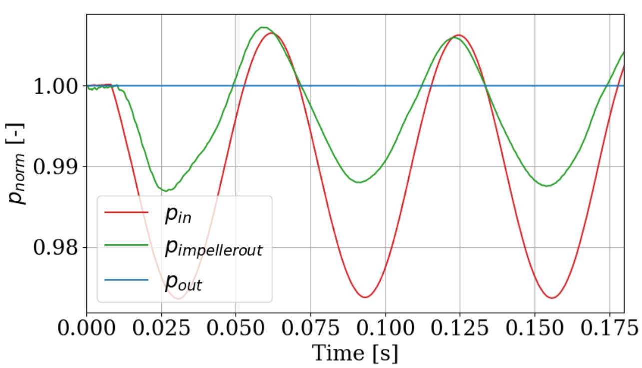


12b) EGR Gen2 Static pressure pulsations

**FIGURE 12:** EGR GEN2 NORMALIZED TOTAL PRESSURE a) AND PRESSURE b) (INLET, IMPELLER-DIFFUSER INTERFACE AND OUTLET)

A particularly notable feature is the reduced amplitude of both total and static pressure fluctuations at the impeller-diffuser interface. Unlike in EGR GEN1, these signals do not closely follow the pressure variations at the impeller inlet. This suggests a damping effect in the EGR GEN2 configuration, likely due to more favorable flow guidance and reduced sensitivity to inlet pulsations.

The high-frequency fluctuations observed in both compressors at the impeller–diffuser interface, highlighted in green in figures 11 and 12, are associated with the onset of flow separation within the impeller, which ultimately progresses to rotating stall.

### 3.6 Subcomponent transient loss generation

An investigation into the mechanisms of flow losses has identified the origins of additional transient losses that determine the curvature of the subcomponent losses providing explanatory insight into potential sources of inefficiency. These phenomena are particularly critical under pulsating flow conditions and should be mitigated to enhance compressor performance.

**Diffuser**

In the parallel diffuser of the EGR GEN1 system, a recirculation zone is observed near the volute tongue even under steady-state conditions. This backflow intensifies during pulsating operation. At high mass flow rates, the backflow constitutes approximately 0.2% of the total mass flow, consistent with steady-state simulation results. However, under low flow conditions, this value increases threefold, reaching up to 0.6% of the total flow. The backflow predominantly occurs along the shroud across the full circumference, with a pronounced concentration in the high-pressure region adjacent to the volute tongue (refer to Figure 13). This recirculation is a primary contributor to the initial transient flow losses. The correlation between increased backflow and elevated total pressure drop at the diffuser outlet under low flow conditions (Figure 11b) substantiates this interpretation. Consequently, the elevated loss coefficient observed during low mass flow scenarios is attributed to this mechanism. Furthermore, the inherently unstable characteristic of the diffuser under these conditions necessitates a higher pressure rise, which in turn imposes an additional pressure load at the impeller outlet during pulsations. In contrast, the EGR_GEN2 configuration, featuring a significantly smaller and more constrictively designed diffuser (lower diffuser area ratio), exhibits no observable backflow under either steady or transient conditions.

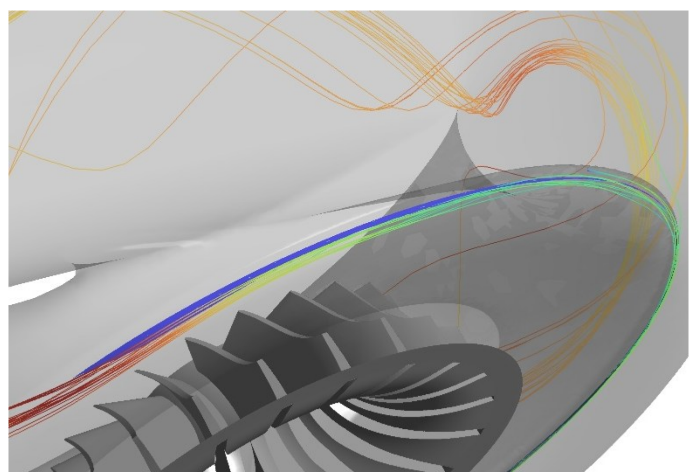

**FIGURE 13:** BACKFLOW AT DIFFUSER OUTLET (BLUE) AS ADDITIONAL LOSS SOURCE (EGR GEN1)

**Volute**

The volute also contributes to additional losses during transient pulsating operation. These losses are primarily induced by variations in flow angle and mass flow rate at the volute inlet.

### Impeller

During pulsating flow conditions, the impeller experiences elevated static outlet pressure, especially under low flow regimes in Figures 11b) and 12b). Given that the pressure rise capability of the EGR GEN1 impeller is near its operational limit, the impeller responds by forming localized stall cells. These stall cells develop predominantly at low inlet pressures, where the required pressure rise is highest. The formation of stall cells extending nearly into the inlet are visible in Figure 14.

The formation of stall cells introduces additional flow losses and blockage, leading to a reduction in mass flow and contributing to the hysteresis observed in the impeller's performance. Due to the limited pressure rise capability, these stall cells propagate significantly upstream within the impeller passage.

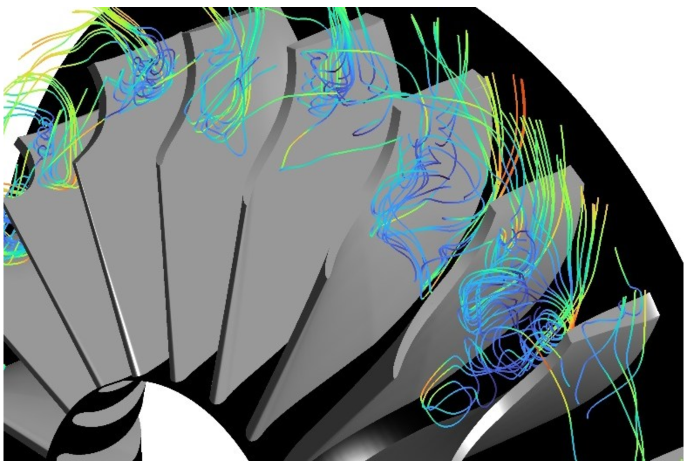

**FIGURE 14:** IMPELLER (EGR GEN1) STALL CELLS DUE TO FLOW PULSATIONS

## 4. DESIGN GUIDELINES FOR COMPRESSORS OPERATING UNDER PULSATING INFLOW CONDITIONS

Based on the findings obtained during the development of the next-generation EGR (Exhaust Gas Recirculation) compressors, several general design principles can be established for compressors subjected to pulsating inflow conditions:

1. **Surge Margin Considerations**
   Irrespective of the inflow characteristics, it is essential to design the compressor with a sufficiently high surge margin. This ensures stable operation and minimizes the risk of flow instabilities and performance degradation. In the presence of inlet pulsations, an additional surge margin, beyond what is typically selected, is beneficial.
2. **Component-Level Stability**
   To achieve overall system stability, each individual subcomponent—namely the impeller, diffuser, and volute—must exhibit stable performance characteristics. The aerodynamic design of these elements should be optimized to prevent local flow separation and unsteady behavior.
3. **Transient design approach**
   Compressor designs intended for operation under inlet pulsation conditions must explicitly account for these pulsations during the design process. A design approach based solely on steady, time-averaged inlet pressure operating points is unlikely to yield a robust and stable compressor.

## 5. CONCLUSION

This study presents a comparative performance analysis of two generations of Exhaust Gas Recirculation (EGR) compressor operating under pronounced pulsating inflow conditions. The first-generation compressor, designed using conventional steady-state methodologies, was unable to maintain a consistent mass flow rate under pulsating conditions. Although the second-generation compressor was specifically engineered to accommodate inlet pulsations, it still exhibited a slight reduction in mass flow.

Key findings:

- **Impact of Pulsations:** Inlet flow pulsations lead to reduced mass flow rates, primarily due to increased average flow losses within the diffuser and volute. These losses arise from convex loss characteristics, where the time-averaged loss exceeds the steady-state loss, a phenomenon explained by Jensen's inequality. Furthermore, an unstable diffuser characteristic contributes to deviations from steady-state predictions. For pulsating flow regimes, maximizing the impeller's static pressure rise is critical. This enhances the overall stage stability, promotes more uniform diffuser flow, and mitigates instabilities near surge conditions.

- **Design Stability:** All subcomponents should exhibit stable performance characteristics under pulsating conditions. Instabilities in individual components amplify flow losses and further reduction in mass flow.

- **Loss Characteristic Robustness:** Loss characteristics, expressed as a function of flow angle ($\alpha$) and mass flow, should be as broad as possible to ensure resilience against flow fluctuations.

- **Design Methodology:** For highly transient flow conditions, a purely steady-state design approach is insufficient to achieve the desired transient operating point.

Based on these insights, a new generation of EGR compressor has been developed, optimized to handle pulsating inflow conditions with enhanced stability and improved performance.

## ACKNOWLEDGEMENTS

We would like to express our sincere gratitude to **Joergen Lyquist**, **Claus Smits Hansen**, **Jesper Pedersen** and **Sofia Grave** from the Howden Helsingoer R&D Team for their exceptional contributions and dedication in implementing the new design into the machine. We also extend our heartfelt thanks to **Matthias Wiegand** and **Thomas Schöneberg** for their invaluable support during the testing phase. Their expertise, innovative ideas, and rigorous efforts have significantly enhanced the quality and impact of this work.

## REFERENCES

[1] International maritime organization IMO, updated 1997, Marpol Convention Annex VI Prevention of Air Pollution from Ships, Nitrogen Oxides (Nox) – Regulation 13.

[2] Benett, S., 2004, Medium/Heavy Duty Truck Engines, Fuel & Computerized Management Systems 2nd edition ISBN 1401814999

[3] Soholt, N., 2020, EGR offered for Dual-Fuel ME-GA Engine, MAN Press release

[4] Howden Turbo GmbH, https://files.chartindustries.com/Howden_EGRCompressor_Brochure.pdf, 2025

[5] Kim, Y., Engeda A., Aungier R., Direnzi G., The influence of inlet flow distortion on the performance of a centrifugal compressor and the development of an improved inlet using numerical simulations, IMech 2001

[6] Roclawski, H., Gugau, M., Böhle, M., CFD Analysis of a Radial Turbine during Load Step Operation of an Automotive Turbocharger, 16th International Symposium on Transport Phenomena and Dynamics of Rotating Machinery, Honolulu, Hawaii, USA, 2016

[7] Hoshi, T., Fujita, Y., Yokoyama, T., Ebisu, M., Development of high.performance turbocharger turbine under exhaust pulsation for next-generation hybrid vehicles, Mitsubishi Heavy Industries Technical Review, Vol 60, 2023

[8] Mosca R., Numerical investigation of Radial Turbines Subject to Pulsating Flow, KTH Royal Institute of technology, Stockholm, Sweden, Doctoral thesis in engineering mechanics, ISBN, 978-91-8040-362-7, 2022

[9] Hayashi, Y., Parikh, A., Barrera-Medrano, M., Martinez-Botaz, R., Hysteresis Effect of Volute on Compressor Performance under Pulsating Flow condition, Proceedings of the ASME Turbo Expo 2023, Boston, USA, GT2023-102332, 2023

[10] Asanaka, Y., Effect of Pulsating Flow on Surge Frequency of a Turbocharger Compressor, J. Phys.: Conf. Ser. 1909 012084

[11] E. M. Greitzer; Internal Flow; Cambridge University press; 2010; ISBN: 9780511616709

[12] Clark, J., Grover, E.; Assessing Convergence in Predictions of Periodic-Unsteady Flowfields; Proceedings of the ASME Turbo Expo 2006; GT2006-90735

[13] R. Hunziker and G. Gyarmathy. The operational stability of a centrifugal compressor and its dependence on the characteristics of the subcomponents. ASME J. of Turbomachinery, 116, 1994

[14] Z. Spakovszky, C. Roduner; Spike and modal inception in an advanced turbocharger centrifugal compressor, ASME Journal of Turbomachinery, 131, July 2009

[15] B. Benneke; A methodology for centrifugal compressor stability prediction; Massachusetts institute of technology, 2009

[16] J. Stemmermann, L.M. Reymond, M. Geilich, P. Jeschke; Investigation of the Stability and Surge Limit in an Industrial Centrifugal Compressor with Variable Inlet Guide Vanes; Proceedings of the ASME Turbo Expo 2023; GT2023-101626

[17] J. Jensen; Sur les fonctions convexes et les inequalities entre les valeurs moyennes; Acta math B.30; 1906; doi:10.1007/BF02418571